Finite Element Human Body Models to study Sex-differences in Whiplash Injury: Validation of VIVA+ passive response in rear-impact

Jobin D. John, I. P. A. Putra, Johan Iraeus

Abstract Neck whiplash injury in rear impact is known to affect females more than males. However, there is a lack of female human body models (HBM) to study whiplash. This paper reports the low-speed passive head-neck kinematic response of a new lineup of models representing an average female and an average male, called VIVA+. The female model serves as the baseline model in the HBM lineup, and the male model is a morphed derivative from the base model.

The head-neck kinematics of these two models were evaluated at multiple levels: from cervical spine functional spine unit (FSU) level to head-neck response to mini-sled rear impacts, and finally, whole-body response to rear-impacts. In general, the female FSU were more compliant in moment-rotation responses. In the head-neck mini-sled simulation, the female upper-cervical spine segments responded with more flexion than male segments, resulting in a more pronounced *S-Curve* formation. In the whole-body rear impact, although the head responded with rearward retraction and rotation and so also T1 with smaller magnitudes, these responses showed considerable differences when compared to the experiments. This could be attributed to the uncertainties in posture and anthropometrical characteristics of the post-mortem human subjects.

These evaluations serve as the first step toward providing models to study sex-differences in whiplash injury risks.

Keywords Cervical spine, inertial loading, head-neck kinematics, low-speed impact, sex-differences, whiplash associated disorders.

I. INTRODUCTION

Whiplash injuries, commonly caused by rear impact, is a neck injury that can provoke a range of short-term symptoms but, in some cases, result in long-term symptoms [1]. Even though whiplash injury has been studied for decades, a conclusive answer to what causes whiplash injury has eluded the injury biomechanics community [2]. Some hypotheses proposed for the mechanism of whiplash injury include spinal ganglia or nervous injury from a pressure gradient in the spinal canal, facet joint and capsular ligament injury, intervertebral disc and ligament injury, vertebral artery injury, and eccentric contraction of neck muscles [3]. The uncertainty in injury mechanism also leads to challenges in defining a whiplash injury criterion, although some, like Neck Injury Criteria (NIC) and Nkm, have been shown empirically to correlate with whiplash injuries [4] and are used in consumer testing [5].

Mechanical models of the human body are essential tools to replicate and study human responses in crash scenarios. Physical or numerical crash test dummies, also called anthropometric test devices (ATDs) are examples of such models. These are generally capable of replicating the human response for just one specific crash mode, either a frontal, a lateral or a rear crash mode. Specifically, for rear impacts, the BioRID was designed to replicate the head and spine motion of an average male [6]. ATDs are, however, limited in the physiological responses they can replicate because of design constraints. In addition to being reasonably biofidelic, these models also need to be robust to sustain the crash without breaking. Computational models of human and finite element (FE) human body models (HBM) in particular, offer a detailed alternative to ATDs as they can capture intricate morphological aspects of the human body as well as model non-linear and viscous material response in the tissues [7]. Another advantage of FE-HBMs is the ability to model muscle activations

J. D. John is a Postdoctoral Researcher, I. P. A. Putra is a Ph.D. student, and J. Iraeus (johan.iraeus@chalmers.se, +46317721366) is a Researcher at the Injury Prevention Group, Vehicle Safety Division, Department of Mechanics and Maritime Sciences, Chalmers University of Technology, Gothenburg, Sweden.

that may play a role in whiplash injury mechanisms [8–10]. FE-HBMs also give the flexibility to parametrically explore the influence of the potential factors that can cause injuries, for example, posture, material, and morphological variations [11–14].

The models, including the FE-HBMs, mainly used to design vehicles represent an average male. Additional models, which however, are not used to test whiplash protection systems, represent a small female (representing 5th percentile size) and a large male (95th percentile) [15-16]. Yet, women tend to have a higher risk of whiplash injuries than men [17], meaning that the average male FE-HBM representation may not be sufficient to develop countermeasures. The differences in injury risk between the sexes and consequent challenges in ensuring the same effectiveness of countermeasures for males and females [18], may indicate the need for a female model that is representative of a larger proportion of women in the population than the 5th percentile small female model currently does. There have been a few attempts at building ATDs and FE-HBMs representing an average female. The EvaRID was designed as an average female counterpart to the BioRID dummy [19]. The ViVA FE-HBM was designed as a simplified model with detailed cervical spine representation intended for whiplash investigations [20-21]. The original VIVA model has recently been rebuilt with a much higher resolution and also morphed into a male counterpart [22]. This newly developed lineup of FE-HBMs is called VIVA+.

As a first step toward using female and male models to study whiplash injury, the objective of this study was to evaluate the passive kinematic response of the head-neck in the VIVA+ finite element human body models. The aim of this paper is to evaluate the cervical spine segmental responses and head rotation and retraction in low-speed rear-impact loading.

II. METHODS

Overview of the Models

The VIVA+ model lineup consists of models representing an average female and an average male. A brief overview of the models is given here. Details of the development and workflow is provided elsewhere [23]. The anthropometry for the HBMs were based on the recommendations from [16]. The female model represents a person with a stature of 1.62 m and a body mass of 62 kg, while the corresponding measures for the male were 1.75 m and 77 kg. The average age for European adults of 50 years was also considered for the external shape of the body. Statistical shape models defined by these anthropometric parameters were used to develop the HBMs [24-25]. The internal skeletal geometries of ribs, pelvis, and lower extremity long bones were also based on statistical shape models [26–29]. The geometries of the remaining skeletal parts were defined by scaling the geometry of the original VIVA model [20]. Skeletal landmark predictions from the statistical shape models were used as a reference to assemble the skeletal components using a rigid registration algorithm [30]. A new hexahedral mesh was developed on these skeletal structure geometries and surrounding soft tissues, except the head and neck, which were morphed and adapted from previous models [20]. The spinal column was assembled based on the C7-T1, T12-L1, and L5-S1 joints landmarks from the statistical outer shape models. Thoracic and lumbar spinal curvatures were defined with respect to these landmark points, also using the curvature information from the outer surface of the skin, while the cervical spine curvature was defined based on a statistical model of the cervical spine in seated vehicle occupants [31].

All model development was done on the female. The male model was created as a derivative model through radial basis function-based mesh morphing [32]. This meant that both the female and male models shared the same model definitions, except the nodes, enabling a consistent definition between the models. For the male model the vertebral shapes were kept, while the size was scaled separately for the thoracic and lumbar regions to match the C7-T1, T12-L1, and L5-S1 joint landmarks from the statistical outer shape models. The cervical spine curvature change was controlled using the parametric model [31].

Head-Neck Kinematics

The kinematics of the head-neck complex was evaluated at multiple levels: at the functional spine unit (FSU) level, at the isolated head-neck level, and at the whole body level.

At the FSU level, the model responses were validated for quasi-static flexion-extension, axial rotation, and lateral bending. For these simulations, each FSU was constrained in a *potting*, where the cortical bone was constrained to the potting using **CONSTRAINED_SHELL_IN_SOLID_PENALTY,* see Figure 1a. The potting material

was modelled as linear elastic with Young's modulus of 2GPa. Different angular velocities were initially tested to ensure that the loading velocity was low enough to guarantee negligible inertia forces, similar to the quasi-static test condition. The reaction moments were measured from the fixed boundary condition. The moment-rotation responses of the FSUs were compared to experiments from [32-34]. The axial rotation and lateral bending responses were compared to[33]. The FSU simulations were run in LS-DYNA R11.0 (Ansys LST, CA, USA).

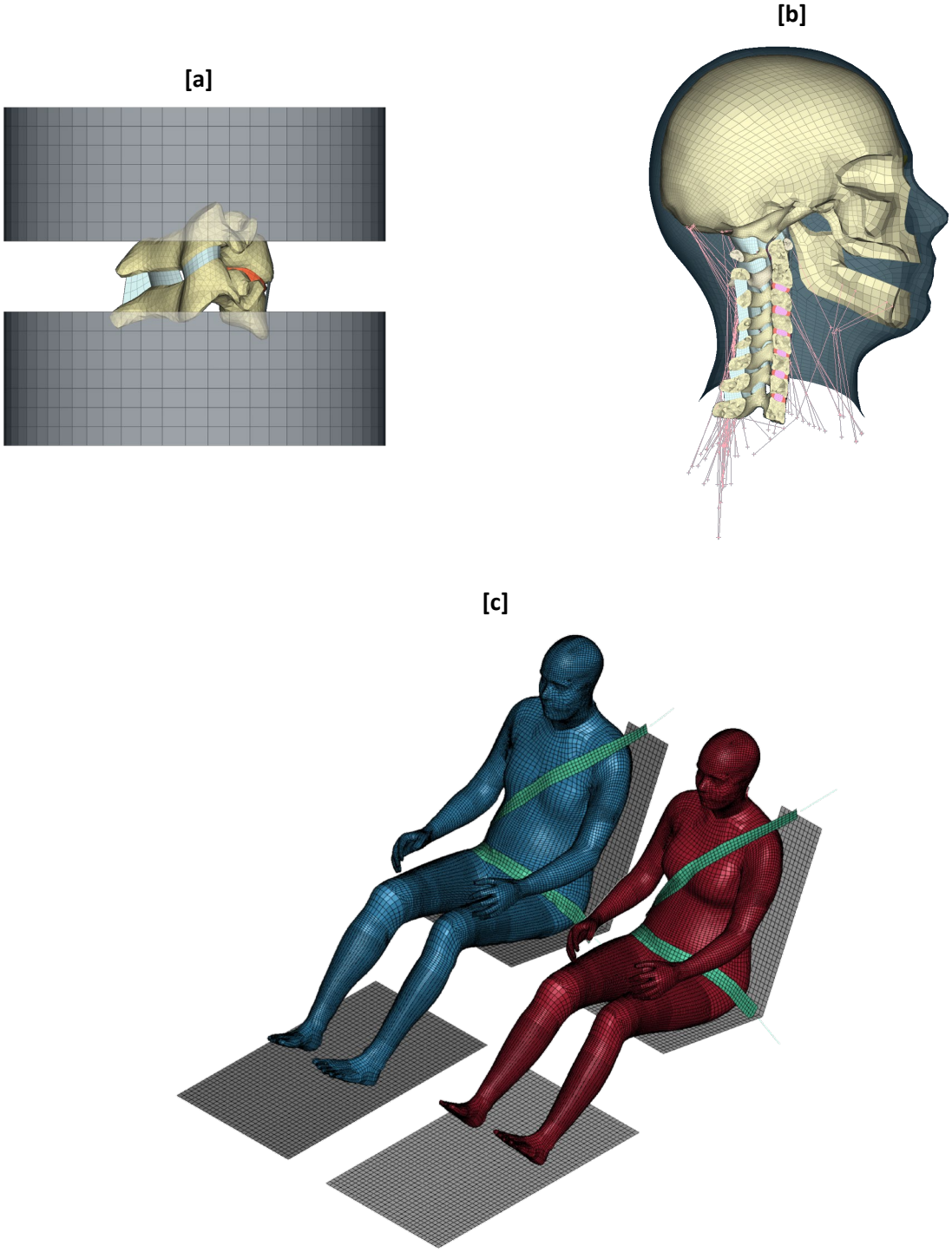

Fig. 1. Models used in this study with their simulation setup. [a] C4-C5 functional spine unit, with quasi-static rotational velocity applied on the superior vertebra and reaction moment measured on the fixed inferior vertebra. [b] Head-neck sub-model (neck soft tissue hidden for clarity). The inferior end of the neck 2D-muscles was constrained to move with T1. [c] The female and male models after gravity settling on the rigid experimental seat.

At the head-neck level, intervertebral rotations were compared with post-mortem human surrogate (PMHS) head-neck mini-sled experiments by [34,35]. A sub-model was created by isolating only the head and neck for

these simulations, see Figure 1b. A rotational rigid-body transformation of negative 9 degrees about the y-axis was applied on the head-neck sub-model to match the OC and T1 orientation in the experiment, as in the physical tests OC was located directly superior to the T1, while the VIVA+ models represent a normal driver posture. The soft tissue mesh at the T1 level and the inferior cervical muscle endings were constrained to the T1 bone to replicate the experimental potting. Posteroanterior acceleration corresponding to 2.6 m/s was applied on the T1 bone. Head rotation, retraction and segmental rotations were compared to the responses from the physical tests.

On the full-body level, head and T1 kinematics were compared to PMHS rear impact experiments by [36]. The full model was gravity-settled on a rigid seat to reach a quasi-equilibrium after 350ms, see Figure 1c. Critical mass-weighted damping was used during this settling phase, using a damping constant *(VALDAMP)* of 0.02922, calculated based on the lowest eigenfrequency of the undamped oscillation. Additionally, the head rotation and anterior-posterior motion were constrained to prevent the head from falling over during the gravity settling. Next, at 350ms, acceleration pulse was applied on the seat, corresponding to the acceleration pulse for change in velocity of 4.4 m/s and 6.8 m/s from the physical tests. The seat belt was modelled using linear elastic material properties (E=2.48 GPa), as a combination of 1D and 2D elements (w=47 mm, t=1.25 mm) [20]. In the experiments, some tests were performed with a foam of 38 mm on the seatback. This was not modelled in the simulation, as it didn't show any considerable influence in the responses. The head rotation and displacement with respect to T1 and the T1 kinematics with respect to the seat were compared with the PMHS experiments. The head displacement in the posterior-anterior direction and inferior-superior direction was measured at the Occipital Condyle with respect to a local coordinate system defined at T1. The origin of the local coordinate system was located on the mid-sagittal section of the anterior-superior edge of the vertebral body. The positive direction of the x-axis was oriented from the posterior edge of the spinous process to the origin. The z-axis was oriented perpendicular to the x-axis in the mid-sagittal plane. The influence of the initial position of T1 and Head relative to the seat back was compared with a posture where the torso was tilted 5 degrees forward with respect to the baseline simulations. Quantitative comparison of the simulation and experimental responses were performed using CORA v3.6.1. The head-neck and whole-body simulations were run using LS-DYNA R9.3.1 (Ansys LST, CA, USA).

III. RESULTS

The FSU level flexion-extension responses for the female and male models are compared with the experimental corridors in Figure 2. All the segmental levels showed responses comparable to the experiments, except the flexion response of C5-C6, which is too stiff. The axial rotation and lateral bending responses of the FSUs are given in the Appendix (Fig. A1 and A2).

The intervertebral rotations of the cervical spine segments and head retraction and rotation in the head-neck mini-sled rear-impact simulation, are shown in Figure 3. The upper cervical spine segment responded with a later extension than the lower cervical spine segments resulting in the 'S-curve formation'. The female upper cervical spine segments responded with more initial flexion than the male segments resulting in the S-curve being more prominent in the female cervical spine. The extension in the lower cervical spine segments was also higher in the female model. The male head showed lower rotation and retraction than the female head in this simulation.

The head-neck responses for whole-body PMHS rear impact simulations are shown in Figure 4. The VIVA+ head rotates with respect to T1 approximately as much rearwards (40°compared to 40°-60°, excluding the outlier) as in the PMHS tests. However, in the PMHS tests, the head initially rotates forward between 50 and 100 ms, resulting in a phase shift compared to the simulation results. Similar behaviour can be seen for the occipital condyles x-displacement with respect to T1. The occipital condyles move about 30 mm in the downward direction with respect to T1 in the simulations, while the PMHS heads move 20-40mm upwards and stay more or less at the same level during the impact. VIVA+ predicts much lower T1 rotation and x-displacement compared to the PMHS tests, while the prediction of z-displacement is in line with the PMHS results. The responses of the models improved when the head and neck were placed in a relatively forward posture compared to the baseline (Figs. A3, A4). The CORA scores for the simulations are given in Tables 1 and A1.

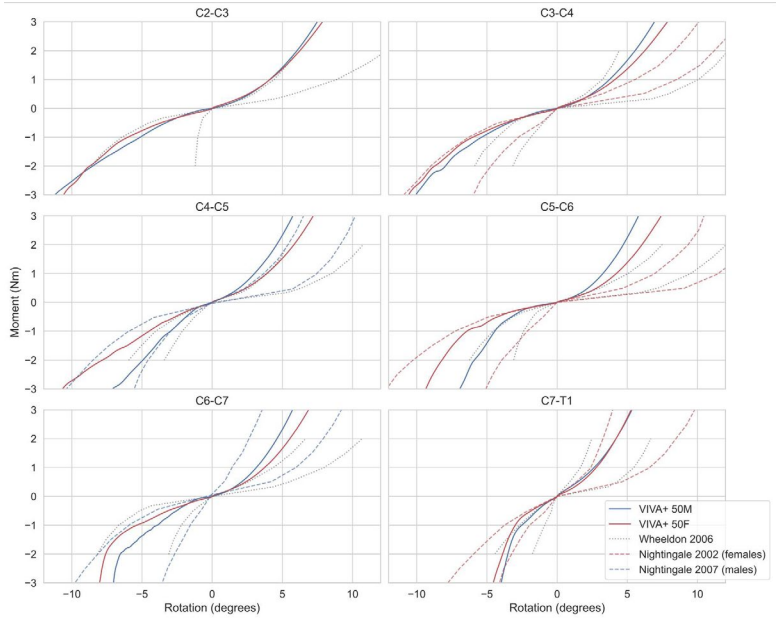

Fig. 2. Flexion-extension response of the cervical spine functional spine units, compared to experimental corridors of PMHS functional spine units. Red curves correspond to female responses and blue curves to male responses.

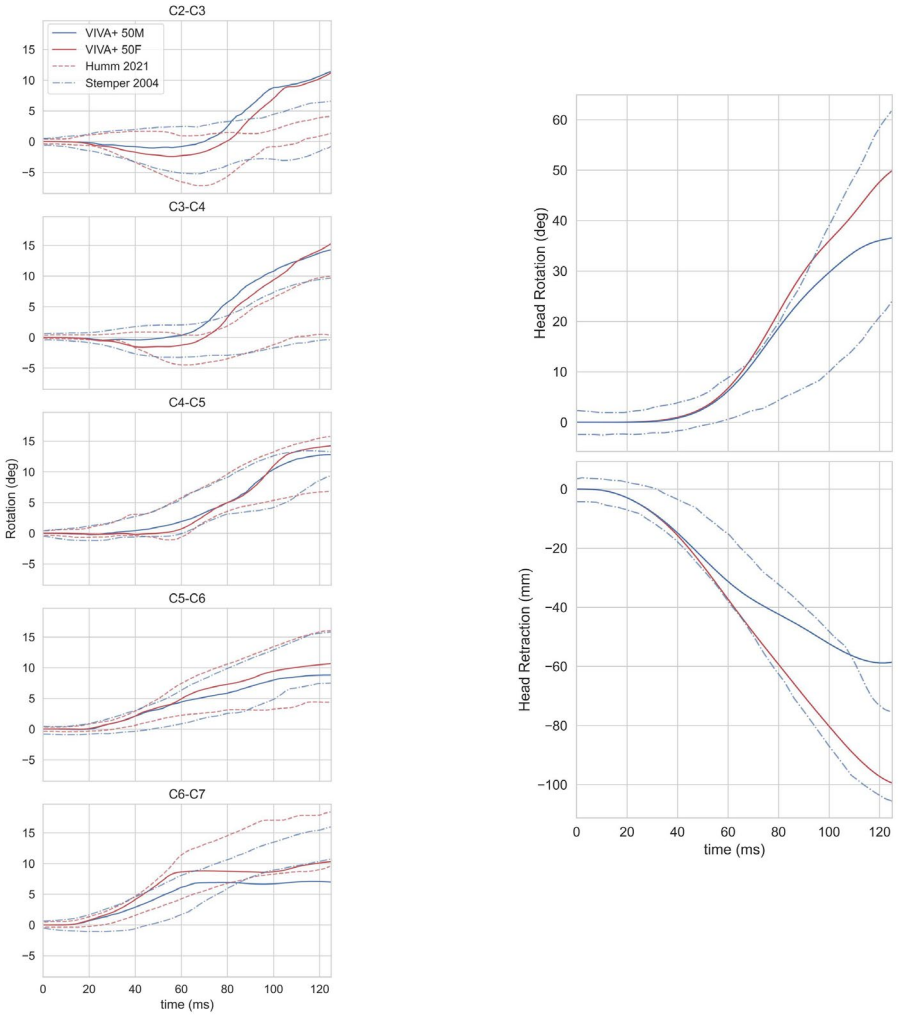

Fig. 3. (Left) Intervertebral rotation of cervical spine segments, compared with experimental responses from PMHS head-neck mini-sled experiments (Stemper et al. 2004, Humm et al. 2021). A positive angle indicates extension of the segments and negative flexion. (Right) Head rotation and retraction compared to PMHS responses from Stemper et al. 2004. Red curves correspond to female responses and blue curves to male responses.

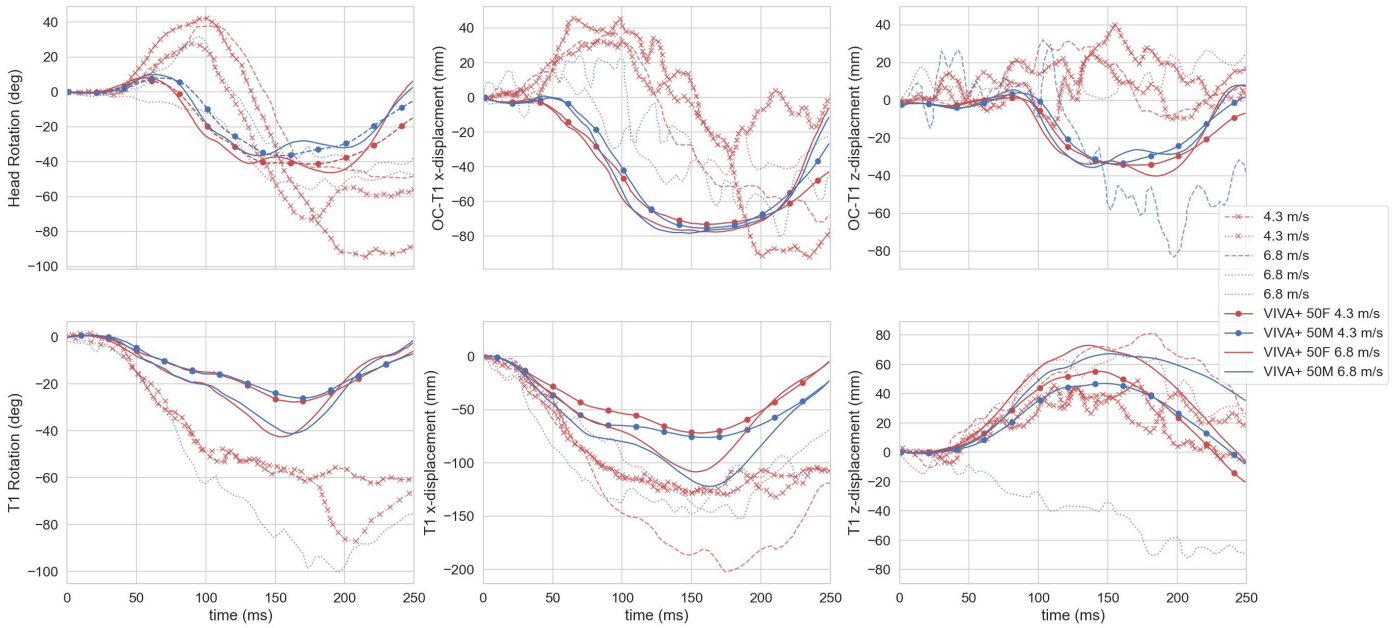

Fig. 4. Head kinematics with respect to T1 (top row) and T1 kinematics (bottom row) with respect to seat at 4.3 m/s and 6.8 m/s rear impacts, compared to PMHS responses from [36]. Dashed lines represent experiments on the rigid seat, and dotted lines represent experiments with the foam on the rigid seat. Red curves correspond to female responses and blue curves to male responses.

TABLE 1
CORA SCORES OF MODEL RESPONSES COMPARED TO PMHS RESPONSES FROM [36]

Kinematics	VIVA+	4.3 m/s	6.8 m/s
Head Rotation	Female	0.44	0.13
	Male	0.46	0.13
OC-T1 x-displacement	Female	0.18	0.31
	Male	0.20	0.32
OC-T1 z-displacement	Female	0.17	0.23
	Male	0.18	0.28
T1 Rotation	Female	0.54	0.48
	Male	0.54	0.53
T1 x-displacement	Female	0.55	0.60
	Male	0.60	0.69
T1 z-displacement	Female	1.00	0.69
	Male	0.88	0.76

IV. DISCUSSION

This study evaluated the head-neck kinematics of the VIVA+ average female and male FE-HBMs in low-speed rear-impact scenarios. The modelling strategy implemented in VIVA+ HBMs helps to generate comparable models, minimising modelling artefacts from mesh-related changes and ensuring that variations in model responses could be attributed to structural variations.

FSU Segmental Rotation

The predicted female FSU responses showed, in general, less stiff behaviour compared to the male FSU responses, following the trend from the experimental range of segmental motions. This was less pronounced in the upper cervical spine (C2-C3, C3-C4) and the C7-T1 joint. Except for the flexion response of C5-C6, all the other responses of the FSUs were comparable to the experimental responses. The sex differences in these

responses come solely from the size variations between female and male models generated from the mesh morphing.

Head-Neck Rear Impact

The *S-Curve* formation is typically seen in rear impacts, where the upper cervical spine segments move into flexion due to the inertia of the head while the lower segments go into extension. This was observed in the head-neck simulations, where the C2-C3 and C3-C4 segments lagged the rest of the segments in extension. The female neck responded with a small amount of flexion in these segments before joining the other segments in extension, while the male neck had comparatively less flexion and only in the C2-C3 segment. This difference in flexion-extension rear-impact response is seen despite C2-C3 and C3-C4 having similar moment-rotation stiffness in the male and female models (Figure 2). The C4-C5 segment, acting as a transition between the upper and lower cervical spine segments, shows similar segmental rotation for the male and female models, as seen in the experiments. In the rest of the lower spine segments, the female spine showed more extension than the male spine, again in line with the experiments.

Two factors can cause the differences seen in these segmental responses. First, the differences in mass of the head between male and female results in different inertial loads during the rear impact. The differences in dimensions of the neck and spinal structures, and particular the difference in neck length can result in different spine moments resulting from the head inertia forces. Second, the differences in vertebral and intervertebral dimensions can result in stiffness variations of the spinal segments. Even though the neck moments from the head inertia forces are expected to be smaller in the female (the head being lighter and neck shorter), the segmental rotations are higher. This may indicate that the smaller dimensions of the spinal column in the females, resulting in reduced stiffness of the spinal column, also have comparatively more influence on the head-neck responses.

Full-body Rear Impact

The rear-impact PMHS experiment analysed in this study was selected for its simple boundary condition with a rigid seat. Although the model head and neck responses showed good correspondence with head-neck mini-sled experiments, the PMHS whole-body response matched less well. In the simulations, the head started retracting with respect to T1 and soon followed with the head rotating in extension as expected in a rear impact. However, in the PMHS study, the head moved forward initially, flexing forward, before retracting and rotating backwards. This behaviour in experimental head kinematics could be explained by the initial posture of the PMHS, as indicated from the sensitivity study of the postures in the models (Fig. A4). A relatively larger distance of the T1 and the head from the seatback resulted in a small forward motion and rotation before the retraction and extension of the head, similar to the experimental response. The T1 anterior-posterior displacement also increased when compared to the baseline simulation. The large T1 rotation of almost 60° (close to 90° in case of 6.8 m/s) and T1 backwards motion of almost 120 mm (up to 200 mm in case of 6.8 m/s) in the experimental responses may indicate the presence of considerable distance between the T1 from the seatback in the experiments. This could also arise from an initial kyphosis of the thoracic spine from the positioning of subjects in the experiments. This would result in a delay between the time of impulse on the seat and T1 engagement, resulting in a delay in the energy transfer to the head through T1, causing the PMHS head to move and rotate forward by the time either the thoracic spine straightens or the T1 vertebra moves ahead of the head. As the VIVA+ models were settled by gravity and the back of the model was in contact with the seat back at the initiation of the sled pulse, the T1 motion of the VIVA+ models could only have a limited backwards rotation and movement with respect to the sled. The vertical motion of the T1 vertebra compared well with the experiments. The HBM head responses, however, are similar in shape and magnitude when compared to other rear-impact experiments [37,38]

Limitations

The model has a simplified solid representation of the neck musculature and associated soft tissues. The neck muscles were represented using two types of elements – 3D elements for compressive behaviour based on adipose tissue properties and 1D muscles representing the tensile response along the muscle fibres. This may not fully capture the interaction of the muscles among themselves and with the vertebral column. The

differences in the responses between male and female models in the study came solely from variations in geometry coming from the mesh morphing and head. Sex-dependent material property variations were not implemented in the current version of the model. Given the considerable differences between the PMHS whole body experiments and VIVA+ responses, more evaluations must be performed with other experimental PMHS and volunteer studies.

Outlook

This study was undertaken as the first step toward further implementing muscle activations in VIVA+ models. The validation of segmental kinematics in rear impact also serves as the basis for the study of spinal canal transient pressure-based injury mechanism of the dorsal root ganglion [39,40]. The male and female models could be further utilised to explore the sex-differences in whiplash injury, using tissue-based injury evaluations and crash reconstructions. Although the differences in the kinematics of the female and male models were modest, these differences could have an influence on the soft tissue responses, such as the facet joint capsular ligaments and nervous structures in the spinal canal.

V. CONCLUSIONS

This study evaluated an average male and an average female passive head-neck responses in low-speed rear-impact inertial loading. In general, the spine segmental responses were comparable to experiments in the FSU and head-neck simulations. The responses in whole body rear-impact simulations are inconclusive and need further evaluations. Although the differences in the kinematics arose from only the geometric and resulting mass differences between the models, the cervical spine showed differences in S-Curve formation during the whiplash motion. Although the differences between the female and male models are modest, it may not be sufficient to represent the female population using an average male model in rear-impact, especially for tissue-based injury studies.

VI. ACKNOWLEDGEMENT

This study was conducted in the VIRTUAL project, funded by the European Union Horizon 2020 Research and Innovation Programme under Grant Agreement No. 768960.

VII. DATA AVAILABILITY

The LS-Dyna simulation input files and postprocessing notebooks are available on OpenVT at https://openvt.eu/fem/viva/publications/2022-john-et-al-ircobi-passive-rear-impact

VIII. REFERENCES

[1] Carroll LJ, Holm LW et al. Course and Prognostic Factors for Neck Pain in Whiplash-Associated Disorders (WAD): Results of the Bone and Joint Decade 2000–2010 Task Force on Neck Pain and Its Associated Disorders. *Journal of Manipulative and Physiological Therapeutics* 2009; 32: S97–107.

[2] Siegmund GP. Soft Tissue Neck Injuries and Other Important Things. *IRCOBI Conference Proceedings*. Athens, Greece, 2018.

[3] Siegmund G, Winkelstein B, Ivancic P, Svensson M, Vasavada A. The Anatomy and Biomechanics of Acute and Chronic Whiplash Injury. *Traffic injury prevention*2009; doi 10.1080/15389580802593269.

[4] Davidsson J, Kullgren A. Evaluation of Seat Performance Criteria for Rear-End Impact Testing BioRID II and Insurance Data. *IRCOBI Conference Proceedings*. Gothenburg, Sweden, 2013.

[5] EuroNCAP. *The Dynamic Assessment of Car Seats for Neck Injury Protection Testing Protocol*., 2021.

[6] Davidsson J, Lövsund P, Ono K, Svensson MY, Inami S. A Comparison of Volunteer, BioRID P3 and Hybrid III Performance in Rear Impacts. *Journal of Crash Prevention and Injury Control* 2001; 2: 203–20.

[7] Cronin DS. Explicit Finite Element Method Applied to Impact Biomechanics Problems. *IRCOBI Conference Proceedings*. Krakow, Poland, 2011.

[8] Putra IPA, Iraeus J, Thomson R, Svensson MY, Linder A, Sato F. Comparison of control strategies for the cervical muscles of an average female head-neck finite element model. *Traffic Injury Prevention* 2019; 20: S116–22.

[9] Kempter F, Kleinbach C, Staudenmeyer M, Fehr J. An Active Female Human Body Model for Simulation of Rear-End Impact Scenarios. *PAMM* 2021; 20: e202000068.

[10] Blouin J-S, Inglis JT, Siegmund GP. Startle responses elicited by whiplash perturbations: Startle responses to whiplash. *The Journal of Physiology* 2006; 573: 857–67.

[11] Corrales M, Cronin D. Importance of the Cervical Capsular Joint Cartilage Geometry on Head and Facet Joint Kinematics Assessed in a Finite Element Neck Model. *Journal of Biomechanics* 2021: 110528.

[12] Corrales MA, Cronin DS. Sex, Age and Stature Affects Neck Biomechanical Responses in Frontal and Rear Impacts Assessed Using Finite Element Head and Neck Models. *Frontiers in Bioengineering and Biotechnology* 2021; 9: 857.

[13] Gierczycka D, Rycman A, Cronin D. Importance of passive muscle, skin, and adipose tissue mechanical properties on head and neck response in rear impacts assessed with a finite element model. *Traffic Injury Prevention* 2021; 22: 407–12.

[14] John JD, Saravana Kumar G, Yoganandan N. Cervical spine morphology and ligament property variations: A finite element study of their influence on sagittal bending characteristics. *Journal of Biomechanics* 2019; 85: 18–26.

[15] Linder A, Svensson MY. Road safety: the average male as a norm in vehicle occupant crash safety assessment. *Interdisciplinary Science Reviews* 2019; 44: 140–53.

[16] Schneider LW, Robbins DH, Pflug MA, Snyder RG. *Development of Anthropometrically-Based Design Specifications for an Advanced Adult Anthropomorphic Dummy Family, Volume 1*. University of Michigan Transportation Research Institute, 1983.

[17] Carlsson A. Addressing Female Whiplash Injury Protection: A Step Towards 50th Percentile Female Rear Impact Occupant Models. 2012.

[18] Kullgren A, Stigson H, Krafft M. Development of Whiplash Associated Disorders for Male and Female Car Occupants in Cars Launched Since the 80s in Different Impact Directions. *IRCOBI Conference Proceedings*. Gothenburg, Sweden, 2013.

[19] Carlsson A, Chang F et al. Anthropometric Specifications, Development, and Evaluation of EvaRID—A 50th Percentile Female Rear Impact Finite Element Dummy Model. *Traffic Injury Prevention* 2014; 15: 855–65.

[20] Östh J, Mendoza-Vazquez M, Linder A, Svensson MY, Brolin KB. The VIVA OpenHBM finite element 50th percentile female occupant model: Whole body model development and kinematic validation. *IRCOBI Conference Proceedings*. 2017: 443–66.

[21] Östh J, Mendoza-Vazquez M, Sato F, Svensson MY, Linder A, Brolin K. A female head–neck model for rear impact simulations. *Journal of Biomechanics* 2017; 51: 49–56.

[22] vivaplus. Publications - VIVA+ Human Body Models. 2022. https://vivaplus.readthedocs.io/en/latest/model/publications/ (accessed April 1, 2022).

[23] John J, Klug C, Kranjec M, Svenning E, Iraeus J. Hello, World! VIVA+: A Human Body Model lineup to evaluate Sex-Differences in Crash Protection. 2022. https://osf.io/uvkjc/ (accessed June 10, 2022).

[24] Reed MP, Ebert SM. *Elderly Occupants: Posture, Body Shape, and Belt Fit*. University of Michigan, Ann Arbor, Transportation Research Institute, 2013.

[25] UMTRI BioHuman: 3D Human Shapes.http://humanshape.org (accessed January 9, 2020).

[26] Brynskog E, Iraeus J, Reed MP, Davidsson J. Predicting pelvis geometry using a morphometric model with overall anthropometric variables. *Journal of Biomechanics* 2021; 126: 110633.

[27] Shi X, Cao L, Reed MP, Rupp JD, Hoff CN, Hu J. A statistical human rib cage geometry model accounting for variations by age, sex, stature and body mass index. *Journal of Biomechanics* 2014; 47: 2277–85.

[28] Klein KF. Use of Parametric Finite Element Models to Investigate Effects of Occupant Characteristics on Lower-Extremity Injuries in Frontal Crashes. 2015. http://deepblue.lib.umich.edu/handle/2027.42/113339 (accessed March 29, 2022).

[29] Klein KF, Hu J, Reed MP, Hoff CN, Rupp JD. Development and validation of statistical models of femur geometry for use with parametric finite element models. *Annals of Biomedical Engineering* 2015; 43: 2503–14.

[30] Hu J. Chapter 10 - Parametric Human Modeling. In: Yang K-H, ed. *Basic Finite Element Method as Applied to Injury Biomechanics*. Academic Press, 2018: 417–45.

[31] Reed MP. *A Parametric Model of Cervical Spine Geometry and Posture*. University of Michigan, Ann Arbor, Transportation Research Institute, 2017.

[32] Zhang K, Cao L et al. An automated method to morph finite element whole-body human models with a wide range of stature and body shape for both men and women. *Journal of Biomechanics* 2017; 60: 253–60.

[33] Panjabi MM, Crisco JJ et al. Mechanical properties of the human cervical spine as shown by three-dimensional load-displacement curves. *Spine* 2001; 26: 2692–700.

[34] Stemper BD, Yoganandan N, Pintar FA. Response corridors of the human head-neck complex in rear impact. *Annual Proceedings. Association for the Advancement of Automotive Medicine* 2004; 48: 149–63.

[35] Humm J, Purushothaman Y, Umale S, Yoganandan N. Segmental Motion Response Corridors of Female Cervical Spines from Gx accelerative loading. *IRCOBI Conference*. Online, 2021.

[36] Yoganandan N, Pintar F. Biomechanics of Human Occupants in Simulated Rear Crashes: Documentation of Neck Injuries and Comparison of Injury Criteria. 2000: 2000-01-SC14.

[37] Deng B, Begeman PC, Yang KH, Tashman S, King AI. Kinematics of human cadaver cervical spine during low speed rear-end impacts. *Stapp Car Crash Journal* 2000; 44: 171–88.

[38] Ono K, Kaneoka K, Wittek A, Kajzer J. Cervical Injury Mechanism Based on the Analysis of Human Cervical Vertebral Motion and Head-Neck-Torso Kinematics During Low Speed Rear Impacts. 1997: 973340.

[39] Yao H-D, Svensson MY, Nilsson H. Deformation of dorsal root ganglion due to pressure transients of venous blood and cerebrospinal fluid in the cervical vertebral canal. *Journal of Biomechanics* 2018; 76: 16–26.

[40] Yao H-D, Svensson MY, Nilsson H. Transient pressure changes in the vertebral canal during whiplash motion – A hydrodynamic modeling approach. *Journal of Biomechanics* 2016; 49: 416–22.

IX. APPENDIX

Lateral Bending of FSUs.

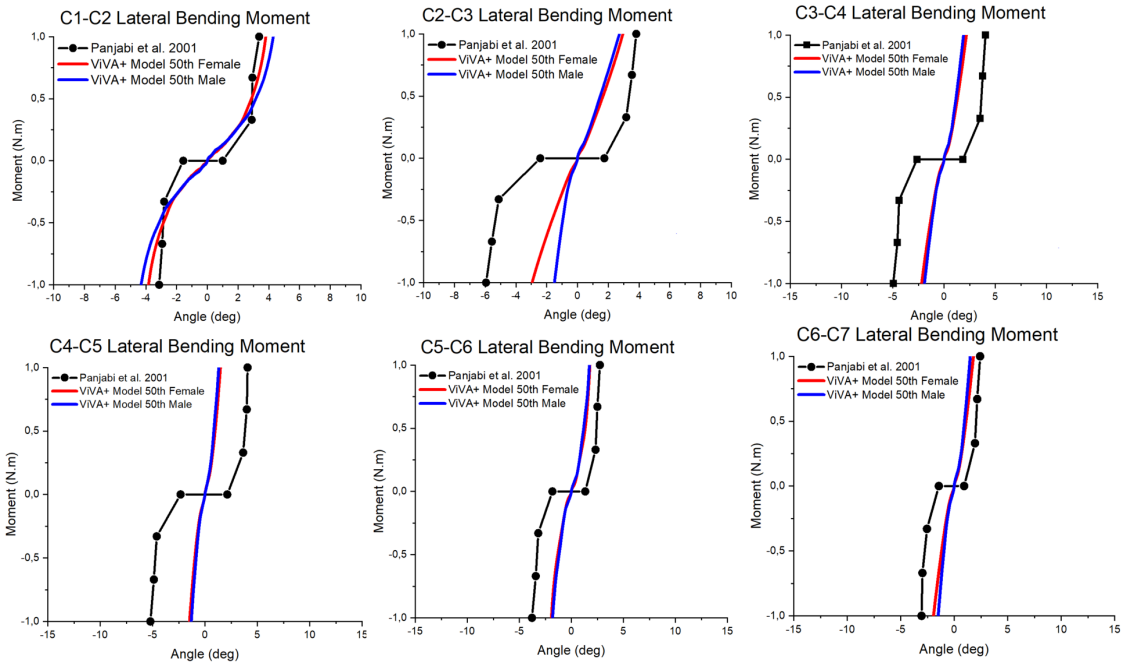

Fig. A1. Moment-rotations responses of FSUs in Lateral Bending

Axial Rotation of FSUs.

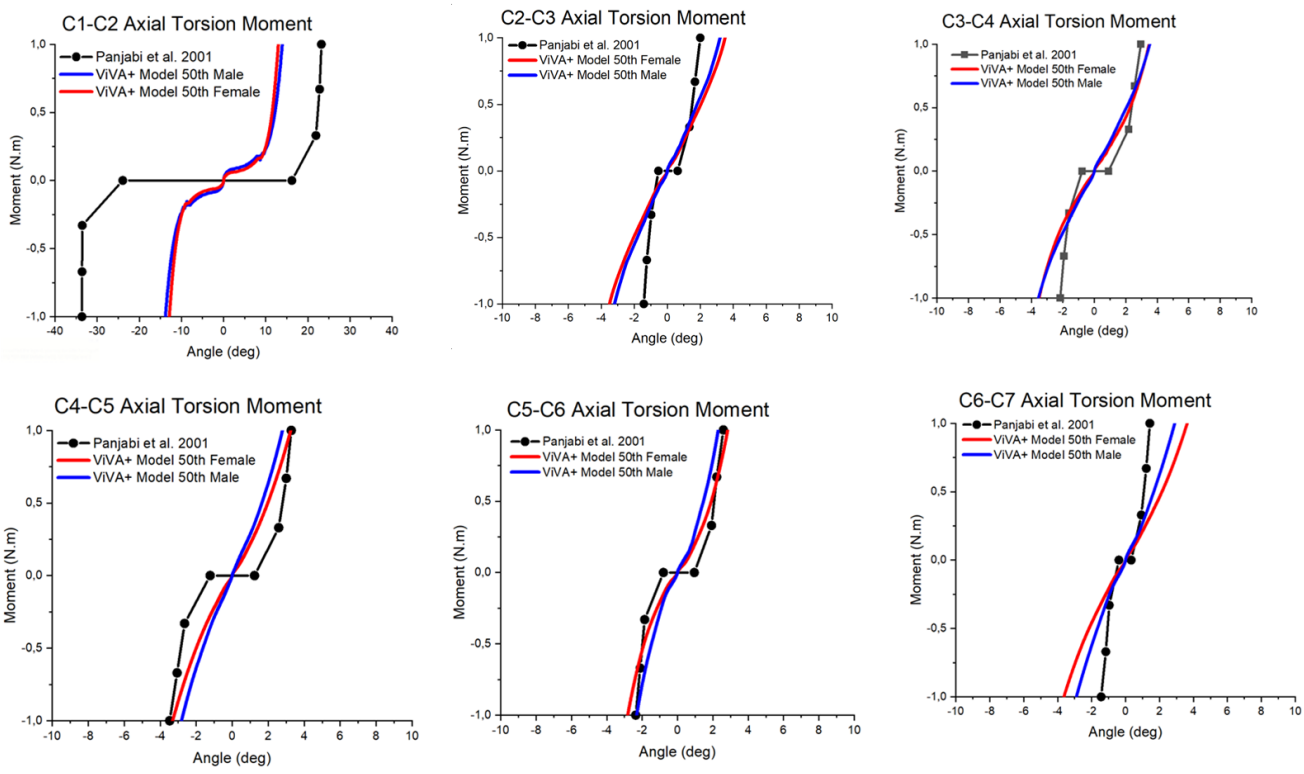

Fig. A2. Moment Rotation response of FSUs in Axial Rotation

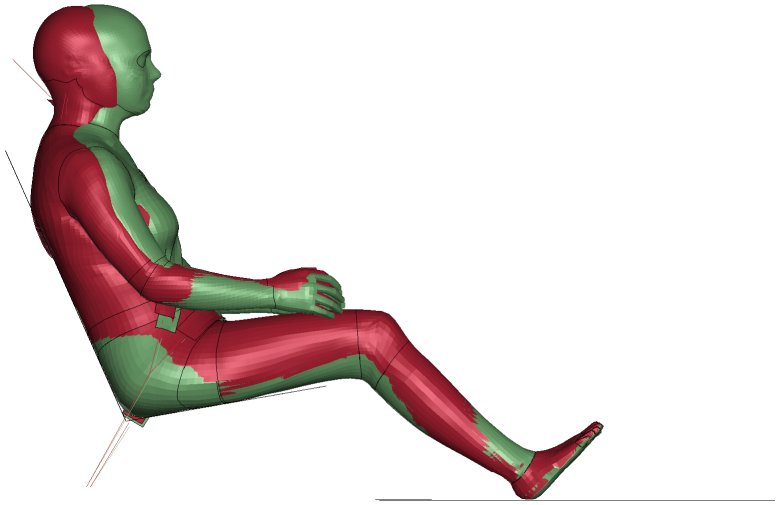

Fig. A3. Sensitivity of the posture was investigated with a forward posture of T1 and Head, as shown in green. The green model has a 5 degrees forward tilt of the torso compared to the baseline.

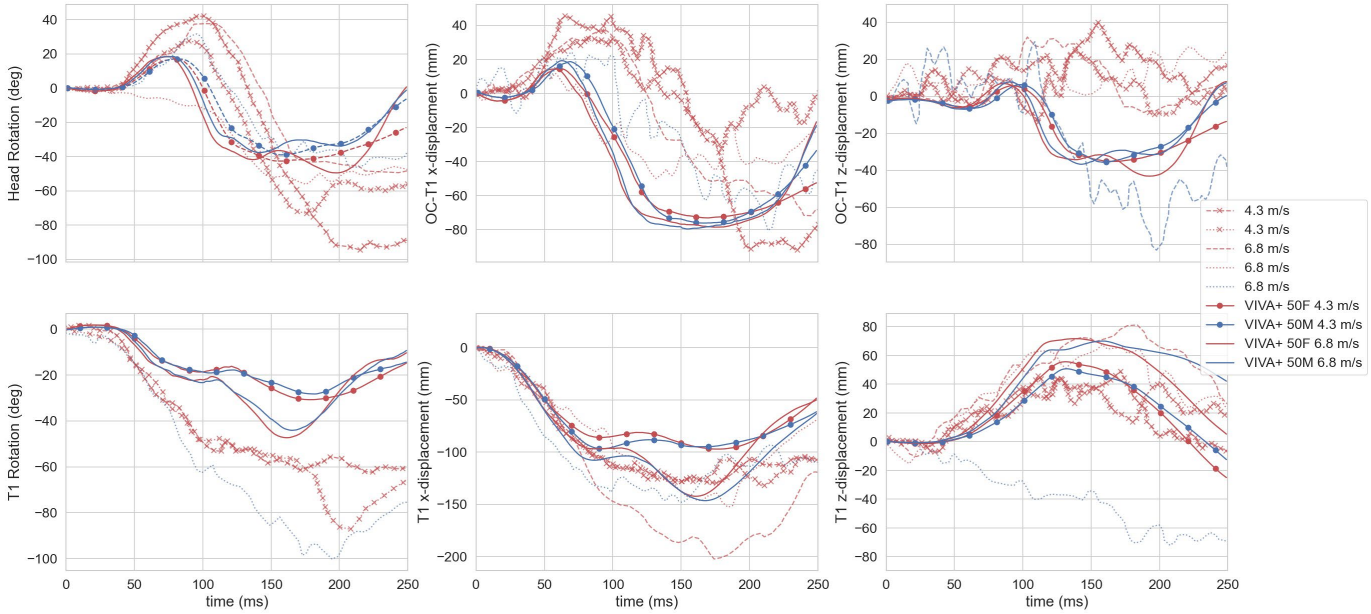

Fig. A4. Head and T1 kinematics for a forward placement of T1 and Head with respect to the back of the sled. The torso had a relative tile of 5 degrees compared to the baseline, as shown in Fig A3.

TABLE A2
CORA SCORES OF MODEL RESPONSES OF FORWARD POSTURE COMPARED TO PMHS RESPONSES FROM [36]

Kinematics	VIVA+	4.3 m/s	6.8 m/s
Head Rotation	Female	0.50	0.13
	Male	0.53	0.13
OC-T1 x-displacement	Female	0.25	0.40
	Male	0.26	0.42
OC-T1 z-displacement	Female	0.19	0.20
	Male	0.18	0.22
T1 Rotation	Female	0.55	0.54
	Male	0.54	0.57
T1 x-displacement	Female	0.71	0.84
	Male	0.60	0.90
T1 z-displacement	Female	1.00	0.66
	Male	0.88	0.71